

Preparation and Properties of Cellulose-Based Nano Composites of Clay and Polypropylene

Jitendra K. Pandey,^{1,2} Sena Lee,³ Hyun-Joong Kim,³ Hitoshi Takagi,² C.S. Lee,⁴ S.H. Ahn¹

¹School of Mechanical & Aerospace Engineering, Institute of Advanced Machinery and Design, Seoul 151-742, South Korea

²Advanced Material Division, Institute of Technology and Science, The University of Tokushima, Tokushima 770-8506, Japan

³Laboratory of Adhesion & Bio-composites, Program in Environmental Materials Science, Seoul National University, Seoul 151-921, South Korea

⁴Division of Materials and Chemical Engineering, Hanyang University, Kyunggi-do 426-791, South Korea

Received 5 January 2011; accepted 24 March 2011

DOI 10.1002/app.34546

Published online 7 February 2012 in Wiley Online Library (wileyonlinelibrary.com).

ABSTRACT: Composites of polypropylene (PP) and crystalline cellulose were prepared after modification of the host matrix by reactive extrusion grafting of maleic anhydride. Acid, alkali, and mechanical treatment of wood flour (WF) was conducted to obtain a suspension of micro- and nanocrystalline cellulose. Layered silicates (clay) were partially intercalated with cellulose crystals, and the modified layered silicate was used as filler in the PP matrix at various concentrations via a melt-blending process. The tensile strength of composites prepared from cellulose-modified clay was greater than that of the PP-clay and PP-WF composites at a 5% filler concentration, whereas deterioration of mechanical properties was observed when clay and WF

were used alone for reinforcement. The dispersion of the filler in the matrix significantly decreased after clay modification with cellulose at higher concentrations, as shown by X-ray diffraction (XRD) data and transmission electron microscopy (TEM) images. Thermogravimetric analysis (TGA) showed an increase in the thermal resistance of samples, which was attributed to the presence of clay platelets that dissipated heat by generating torture paths. © 2012 Wiley Periodicals, Inc. *J Appl Polym Sci* 125: E651–E660, 2012

Key words: biopolymers; nanocomposites; poly(propylene)

INTRODUCTION

The most important advantage of natural fibers as fillers in developing reinforced polymer composites is their eco-friendly nature, compared with traditional carbon and glass fiber-based composites. Disposal of glass or carbon fiber-filled composites, which are synthetic nonbiodegradable polymers, after their useable life has created serious environmental issues.^{1,2} Substitution of glass fibers by natural fibers has advantages, such as being eco-friendly, and many studies have investigated the potential of natural fibers as fillers. Previous results have shown that composite stiffness was sufficient, because natural fibers have high strength and stiffness.³ However, drawbacks, such as poor filler dispersion and incompatibility with the polymer matrix, have also contributed to catastrophic failures of natural fiber

composites. The stress transfer from the polymer matrix to the filler determines the final properties of a composite. Material properties of polymer composites are strongly dependent on the degree of contact between the phases. Unfortunately, natural fiber composites do not attain the same strength as glass fiber composites because of incompatibility between the hydrophobic host polymer matrix and the hydrophilic natural fiber. In addition to the previously mentioned challenges, there are compositional parameters that determine properties, such as filler content, particle size, and the use of coupling agents. The use of thermoplastics reinforced with wood fillers is growing rapidly due to their light weight, stiffness, strength, and economical and ecological processing. Wood flour (WF) is an esthetically pleasing material preferred for use in outdoor decks, railings, fences, landscaping timbers, cladding and siding, park benches, molding and trim, window and door frames, and indoor furniture.² In most of these applications, WF-based composites are used as construction materials in which the load-bearing capacity of the dispersed phase is crucial. Catastrophic failure typically occurs due to debonding of the matrix and filler, generating voids that lead to large cracks. The intensity of debonding stress

Correspondence to: S.H. Ahn (ahnsh@snu.ac.kr.).

Contract grant sponsors: ERC (Micro-Thermal System Research Center), Second Stage of Brain Korea 21 of Seoul National University and Japan Society for Promotion of Science.

depends on particle size and interfacial adhesion. Interfacial interaction can be increased using various coupling agents.⁴ Surface treatment of the wood by sodium hydroxide, silane, and esterification (acetylation, propionylation) is commonly used for interfacial improvement, and polymers functionalized with maleic anhydride (MA) and acrylic acid have also been widely used.⁵

Recently, highly crystalline cellulose (micro/nanocrystalline cellulose, referred to as cellulose whiskers or cellulose crystallites, depending on shape and size) has been shown to enhance material properties at lower filler concentrations than unfilled polymer matrices and their microcomposite counterparts.⁶ Depending on the cellulose source, these micro/nanocrystals have a wide variety of aspect ratios (L/D), ranging from 1 to 100.^{7,8} Wood can be converted into nanodimensional particulates by sequential acid treatments to produce nanocrystals of 100–300 nm lengths and 3–5 nm diameters that can be extracted from soft wood.⁷ Cellulose nanocrystals have been used as fillers in many polymer matrices, such as silk fibroin, cellulose acetate butyrate, starch, polylactic acid, polyvinyl alcohol, and other plastics.^{8,9} However, the extraction of nanofibers overcame drawbacks, such as time-consuming preparation, low yield, and hydrophilicity, before industrial applications.

Recently, polymers filled with nanoscale-layered silicates have shown remarkable improvements in mechanical, thermal, and physicochemical properties compared with pure polymers, even at low filler concentrations if the filler is homogeneously dispersed.¹⁰ These layered silicates have attracted attention because they are cost-effective, readily available, and have high aspect ratios, which increase energy transfer between phases. Exfoliated structures have resulted in the best mechanical properties for polymer matrices. Thus, studies have focused on developing completely individual clay platelets because the clay layers must be forced apart to break their interaction through onium chains to produce an ideal nanocomposite.¹¹

The use of nanosilicate layers combined with cellulose fibers for reinforcement is a new pathway for next-generation materials,¹² and there is interest in investigating synergetic effects between nanoclays and biofillers on the properties of polymer composites.¹³ Thunwall et al.¹⁴ studied the processing and properties of clay-interfaced cellulose fiber composites and concluded that treating the fiber with nanoclay improved the dispersion of fibers and the mechanical performance of the composites. Zhong et al.¹⁵ observed that the addition of less than 5% nanoclay to the wood polyethylene matrix increased the *d*-spacing of the silicate layers, decreased the flexural strength by 24%, and increased the modulus by 10%. Mohanty and coworkers¹⁶ fabricated nanocomposites from cellulose acetate powder, eco-friendly triethyl citrate plasticizer, and organically modified

clay in which the tensile strength and modulus of the cellulosic plastic reinforced with organo-clay improved with decreasing plasticizer content. Oksman and coworkers¹⁷ compared layered silicates and microcrystalline cellulose as nano reinforcers for a polylactic acid matrix and found that the reinforcer significantly impacted the mechanical properties.

This study investigated synergistic effects of reinforced cellulose micro/nanocrystals from wood and layered silicate for polypropylene (PP) composites. PP was selected as a matrix because it is one of the most commonly used polymers in many applications, and it addresses plastic waste problems because it is not eco-friendly. Fourier-transform infrared (FTIR) spectroscopy, scanning electron microscopy (SEM), thermogravimetric analysis (TGA), and X-ray diffraction (XRD) measurements were used to analyze functional group variation, morphology, thermal properties, and the crystalline nature of the composites.

EXPERIMENTAL

Materials

PP was purchased from Hyosung Co., South Korea. It had an MFI of 1.7 g/10 min (190°C/2160 g) and a density of 0.91 g/cm³. WF was purchased from Saron Filler Co. and Dong Yang CMI Co., South Korea. The particle size of the WF was 110 μm. Other chemicals were from Dae Jung Chemicals and Metals Co., Gyeonggi-do, Korea, and they were used after drying and purification when necessary. Cloisite Na⁺ was the nanoclay used in this study and was purchased from Southern Clay.

Preparation of composites

MA-grafted PP (PP-g-MA), used as a compatibilizer, was prepared as follows. First, 5% MA (w/w of PP), 0.05% dicumyl peroxide and PP were dry-mixed and poured into a hopper with a twin-screw extruder. Then, different temperature zones were set from 145 to 180°C. The strands of MA-g-PP were converted into pellets by a pelletizer. These pellets were used as a compatibilizer for PP at a constant concentration of 5%, referred to as PP. Chemical and physical treatments were applied to convert the wood to a microcrystalline filler.¹⁸ WF was soaked in a 0.5% alkali solution for 10 days and boiled for 2 h at 80°C with a 2% NaOH solution, followed by washing with deionized water. Hydrolysis by 65% H₂SO₄ was conducted at 60°C for 30 min followed by centrifugation, sonication, and neutralization. The resulting suspension of cellulose crystals contained a mixture of nano- and micro-crystals, referred to as crystalline cellulose. The silicate layer (cloisite Na⁺)

TABLE I
Compositions of Samples by Percentage

NWC	WF	CL	PP	Samples
5	0	0	95	NWC5
10	0	0	90	NWC10
20	0	0	80	NWC20
0	5	0	95	WF5
0	10	0	90	WF10
0	20	0	80	WF20
0	0	5	95	CL5
0	0	10	90	CL10
0	0	20	80	CL20

was dissolved in water for 2 days to produce a green gel-like colloid solution. The water-dispersed crystalline cellulose was added to the colloid solution of clay at 10 : 90 (clay : cellulose) ratio. The mixture was stirred for 24 h at room temperature, followed by heating for 1 h at 100°C. The suspension was sonicated for 35 min at a 40% power output. This nanowood clay (NWC) was filled in the PP matrix at different loadings using the twin-screw extruder. The extruder barrel was divided into eight zones, and the temperature in each zone was individually adjustable. The temperature of the mixing zone was maintained at 190°C with a screw speed of 250 rpm. The extruded strand was cooled in a water bath and pelletized using a pelletizer. Extruded pellets were oven-dried at 80°C for 24 h and stored in sealed polyethylene bags to minimize moisture. The PP matrix was reinforced with clay and WF under similar conditions at 5, 10, and 20% filler concentrations. The dry pellets were molded for mechanical property measurements by injection molding. The composites of treated WF and layered silicates were prepared for comparison. The different compositions of the samples are shown in Table I.

Characterization techniques

Fourier-transform infrared spectroscopy (FTIR)

Attenuated total reflectance infrared (ATRIR) spectra of the samples were recorded using a FTIR 300E Jasco spectrometer. The incident beam angle was 458°. For each measurement, 60 scans were acquired with a spectral resolution of 4 cm⁻¹. The Win First software (ver. 3.57; Mattson Instruments), was used for acquisition and evaluation of IR spectra.

X-ray diffraction (XRD)

XRD patterns of the samples were acquired using a Rigaku (Japan) diffractometer with Cu-K α radiation at 50 kV and a scan rate of 1°/min. The *d*-spacing was calculated using Bragg's equation with λ at 0.154 nm.

Scanning electron microscopy (SEM)

The small portion of samples after mechanical analysis was dried under vacuum for 24 h at 50°C. The coating of samples was carried out by gold sputtering and was further examined with an electron microscope (DS-130C; Topcon) for morphological changes.

Transmission electron microscopy (TEM)

TEM images of the composites were acquired at an acceleration voltage of 120 kV using a JEOL JEM-2000 EXII TEM. The samples were embedded in an epoxy resin and cured overnight at room temperature. Then, they were then section with a microtome to produce ~70-nm thick sections. Ultrathin sections were prepared with a diamond knife, and final images were captured by placing the samples on carbon-coated 200-mesh Cu grids.

Mechanical properties

The tensile test for the composites was performed according to ASTM D638 using a Universal Testing Machine. The mold with two cavities was fabricated (type V in ASTM 638) and adjusted with an injection-molding machine (G-100T, Morgan Industries). The cylinder temperature of the machine was 190°C, and the mold temperature was 50°C. For each treatment level, five replicates were tested, and the results represent the average of five values. Tensile deformation was determined using an extensometer at a crosshead speed of 10 mm/min.

Differential scanning calorimetry (DSC)

DSC analysis was carried out using a TA Instrument DSC Q 1000 (NICEM at Seoul National University) with 5–10 mg of each composite in an aluminum capsule. Each sample was scanned from 30 to 200°C at a heating rate of 10°C/min, followed by cooling at the same rate under nitrogen atmosphere to prevent oxidation.

Thermogravimetric analysis (TGA)

TGA was conducted with a Seiko (Torrance, CA) model TG/DTA 32 thermal analysis system. The TGA scans were recorded at 10°C/min under a nitrogen atmosphere from 50 to 500°C.

RESULTS AND DISCUSSION

FTIR spectroscopy

The flour was pulverized wood containing amorphous and highly crystalline regions, comprised of

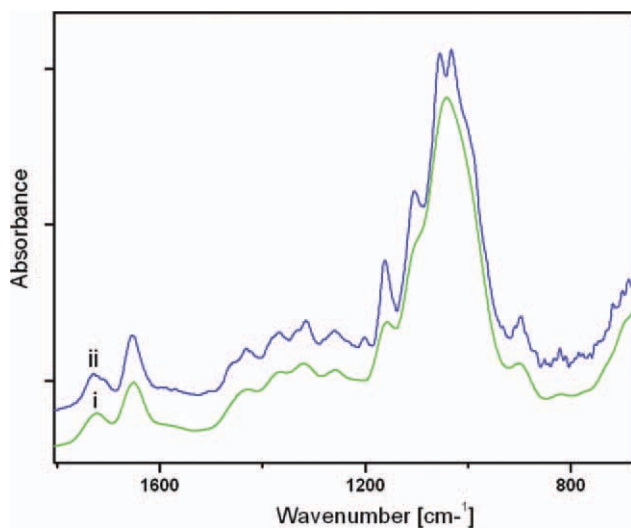


Figure 1 FTIR spectra of treated (i) and untreated (ii) wood flour. [Color figure can be viewed in the online issue, which is available at wileyonlinelibrary.com.]

hemicellulose, lignin, and cellulose. FTIR spectroscopy indicated that cementing material like lignin was removed through various treatments (Fig. 1). Alkaline treatment eliminated lignin, as confirmed by the reduction in the peaks at 1140, 1222, and 1510 cm^{-1} assigned to aromatic skeletal vibrations. This treatment likely caused degradation of aromatic structures, as indicated by diminished peak intensity from 1530 to 1550 cm^{-1} .¹⁹ The peak observed at $\sim 1735 \text{ cm}^{-1}$ was attributed to C=O vibrations and indicated the partial washout of hemicellulose.²⁰ XRD graphs in Figure 2 show three main peaks at ~ 22 , 16, and 34° that correspond to the 200, 023, or 004 and 110 planes, respectively.^{21,22} The relative sharpness of XRD peaks for treated flour was attributed to the high crystalline content. This may have been due to decomposition of the amorphous zone during acid digestion, resulting in highly crystalline regions.^{18,23} The composites showed a slight decrease in the hydroxyl region of the FTIR spectra, which was identical for all NWCs, regardless of filler content. The MA groups, present in the host polymer, decreased the hydroxyl region²⁴ due to association between negative oxygen atoms in the carboxylic groups and hydrogen in the filler. Esterification may have occurred between functionalities of cellulose and the maleated portion of the matrix, as indicated by the appearance of peaks at 1722–1746 cm^{-1} ²¹ in the solution-blended composites in the presence of catalyst. Esterification has also been reported in the melted state, which was facilitated by reaction with activated cellulose containing large amounts of free hydroxyl groups on the surface.⁵ In this study, there was no detectable peak in the ester region. Most of the hydroxyl groups were confined

between platelets of layered silicate and reduced the possibility of reactions with carbonyl groups of MA-grafted polymer chains.

Thermogravimetric analysis

Figure 3 shows the thermal resistance of the samples, which was measured under nitrogen with increasing temperature until 50% of the initial weight was lost. Silicate layers are thought to increase thermal resistance by hindering diffusion of volatile decomposition products or by forming a charred silicate surface that dissipates heat by absorbing it in the inorganic phase.^{2,10} The increased thermal stability of CL5 compared with PP was attributed to the presence of clay, which increased the temperature needed to reach 50% weight loss. The mixing of silicate layers did not enhance the material properties, and the dispersion was not uniform. Increased clay content increased agglomeration inside the matrix, forming large tactoids and macro, phase-separated composites with poor heat resistance, due to low energy dissipation.²⁵ WF composites exhibited poor thermal stability compared with other samples, and initial degradation at 130°C was attributed to the dehydration reaction and degradation of hemicellulose.¹² Furthermore, the poor interfacial adhesion may also have contributed to the degradation. In our previous research, we observed an increase in the thermal stability of bio-flour-PP composites after compatibilization with MA-functionalized PP due to increased intermolecular bonding between the filler and the matrix.²² TGA of different treated and modified WF is shown in Figure 4. Increased thermal stability was observed after mixing with clay, and it decreased after treatment with acid. Cellulose crystals, extracted through acid

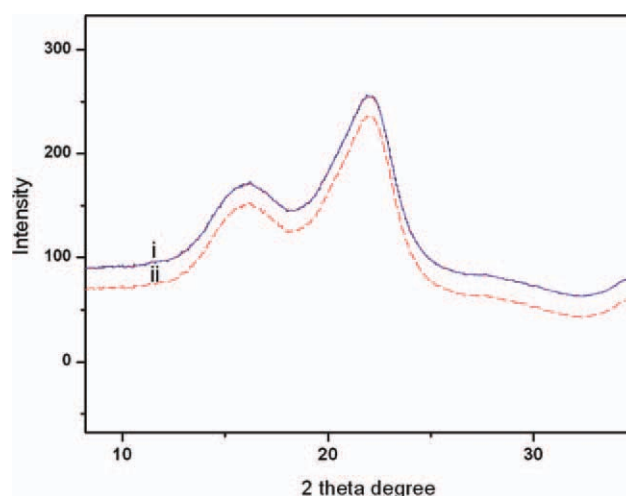


Figure 2 XRD data of treated (i) and untreated (ii) wood flour. [Color figure can be viewed in the online issue, which is available at wileyonlinelibrary.com.]

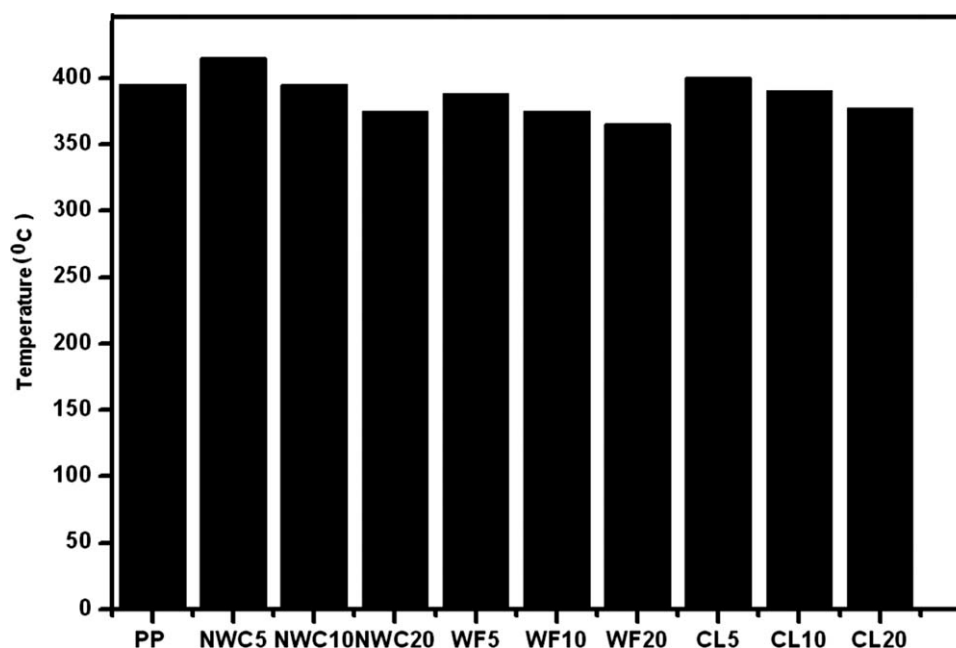


Figure 3 TGA temperature at 50% weight loss.

treatments, have been thought to be less thermally stable than microcrystals because of the large number of free end chains containing sulfate groups.²³ In this study, acid-treated WF was used after neutralization by sequential alkali treatment, and all NWCs exhibited higher thermal stability than the composites with only WF and clay. Thermal stability of NWC5 was better than that of NWC10 and NWC20, possibly due to the individualization of clay platelets that generated more torture paths for thermal diffusion.²⁶ Thus, polymer chains were not quenched uniformly between the platelets for NWC10 and NWC20,

resulting in poor thermal properties and larger particles. Dispersion of silicate layers was more important than the filler concentration in the host matrix for thermal stability, and cellulose crystals may have further reduced the agglomeration of clay tactoids.²⁵

XRD and TEM analysis

The crystalline status of the host polymer in composites defines the mechanical properties. Thus, the crystalline nature and other material properties can be tailored in the resulting hybrid. The properties of nanocomposites are often related to their structures and to the orientation of their particles. Cellulose is a highly crystalline material that forms through degradation of amorphous regions, and XRD data in Figures 5 and 6 suggested the presence of cellulose-I, which likely did not change during processing. The neat clay had a characteristic peak at 7.2° that corresponds to the 2.3-nm interlayer spacing. After mixing with crystalline WF, the peak shifted toward lower angles, indicating increased intergallery distance. The new peak was located at 3.2° and was sharper than the original, indicating that the stacking order was destroyed and platelets moved apart, but maintained order.²⁷ The samples filled with 5% clay modified with cellulose did not show a peak in this region, indicating better dispersion of silicate layers inside the matrix. The reflection peak collected for NWC10 and NWC20 did not show any variation in position, supporting the conclusion that a higher percentage of cellulose-modified clay inside the matrix did not cause further separation of tactoids as it

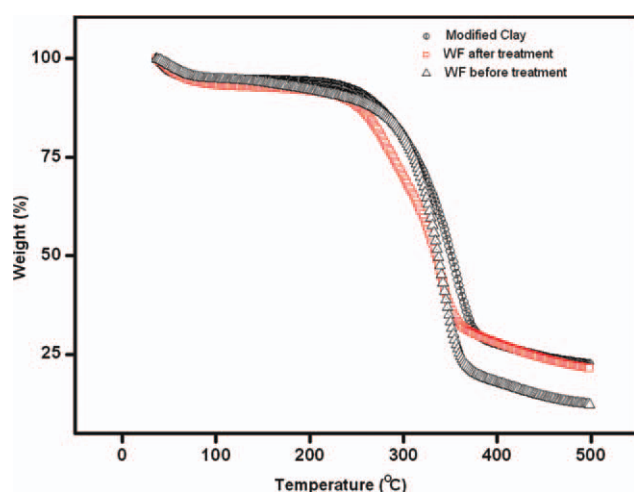


Figure 4 TGA of different wood flour samples showing the effect of clay on thermal stability. [Color figure can be viewed in the online issue, which is available at wileyonlinelibrary.com.]

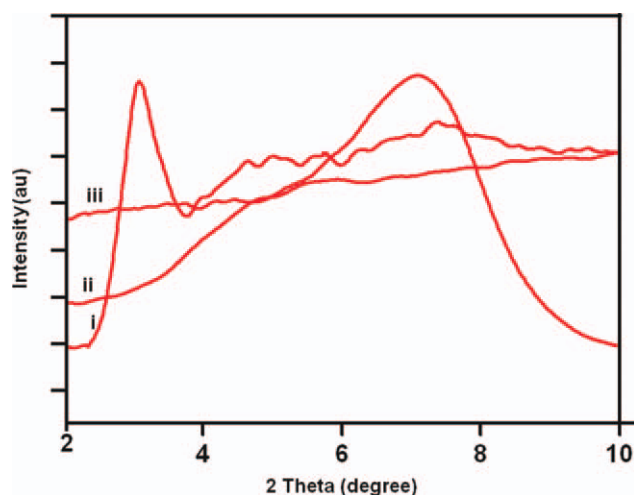


Figure 5 XRD data clay modified with cellulose (i), neat clay (ii), and NWC 5 composites (iii). [Color figure can be viewed in the online issue, which is available at wileyonlinelibrary.com.]

did in NWC5. The TEM images in Figure 7 show that all the samples were more or less similar, and the higher dispersion in NWC5, based on XRD data, was not observed in the TEM micrographs. As mentioned previously, the properties of nanocomposites are related to their structures and to the orientation of polymer chains in the hybrids. The aspect ratio of nanoclays will determine the diffusion of the polymer into silicate layers, especially in the presence of functionalized chains. This results in aligned, dispersed nanoclays in the polymer matrix and a higher melting point when a compatibilizer is used. A complete description of the structure includes the state of exfoliation and intercalation. Generally, the success of nanocomposite preparation is reported using conventional qualitative techniques in which

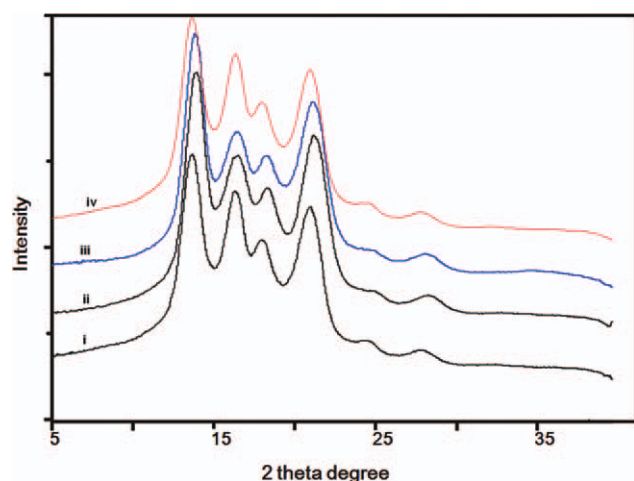


Figure 6 XRD data of composites. i, ii, iii, iv are PP, WFC5, 10 and 20, respectively. [Color figure can be viewed in the online issue, which is available at wileyonlinelibrary.com.]

the volume probed is small and may not represent the entire nanocomposite. Because TEM measurements are taken for small portions of large samples, different dispersion levels of silicate layers can be observed in the same sample. Similar results may explain the present data in which XRD results did not agree with qualitative TEM observations; NWC10 appeared to have better dispersion than NWC5. NWCs samples showed similar dispersion that was better than those for CLs at all concentrations, and these results agreed with XRD data that did not vary for the NWC samples. Although MA-g-PP chains, which were compatible with clay, were present in the matrix, it was not enough to overcome the incompatibility between PP and clay. The good dispersion in NWCs may have been due to additional attraction between MA-g-PP chains and hydroxyl groups of the cellulose fibers. When the concentration of NWC increased from 5 to 20%, agglomeration increased due to greater interaction between filler and filler than between filler and matrix, which reduced the dispersion.

Differential scanning calorimetry (DSC)

The crystallization behavior of the nanocomposites is shown in Table II, and endothermic heat flow data is shown in Figure 8. The samples exhibited single peaks, and PP had a melting temperature (T_m) of 164°C¹⁵. The T_m of the samples increased after reinforcement with cellulose-modified clays and was highest for NWC5. The T_m increased significantly with 10 and 20% NWC concentrations, but was not as high for NWC5. The results indicate that filler dispersion was more important than filler concentration for influencing the melting of polymer chains. Addition of reinforcing phases caused changes in the crystallization temperature and onset temperature for the PP matrix. Cellulose has been shown to nucleate PP and influence transcrystallinity as the size of the spherulites decreased.^{14,15} The WF composites had higher crystallization temperatures at all concentrations, and the peaks were sharper than those of composites prepared by mixing only clay in the matrix. Thus, the nucleating effect of WF was greater than that of clay in these composites. However, it has been reported that when clay is modified with an organic modifier and mixed with PP, it induces crystallization and may act as a nucleating agent.¹⁰ The extent of intercalation between MA-g-PP chains and silicate galleries decreased as clay loading increased. Dispersed clay particles acted as nucleating agents and lowered the spherulite size.²⁶ The increase in crystallization temperature observed for NWC5 was lower than with NWC10 or NWC15. This behavior can be explained by probable encapsulation of crystalline cellulose through the interaction of layered

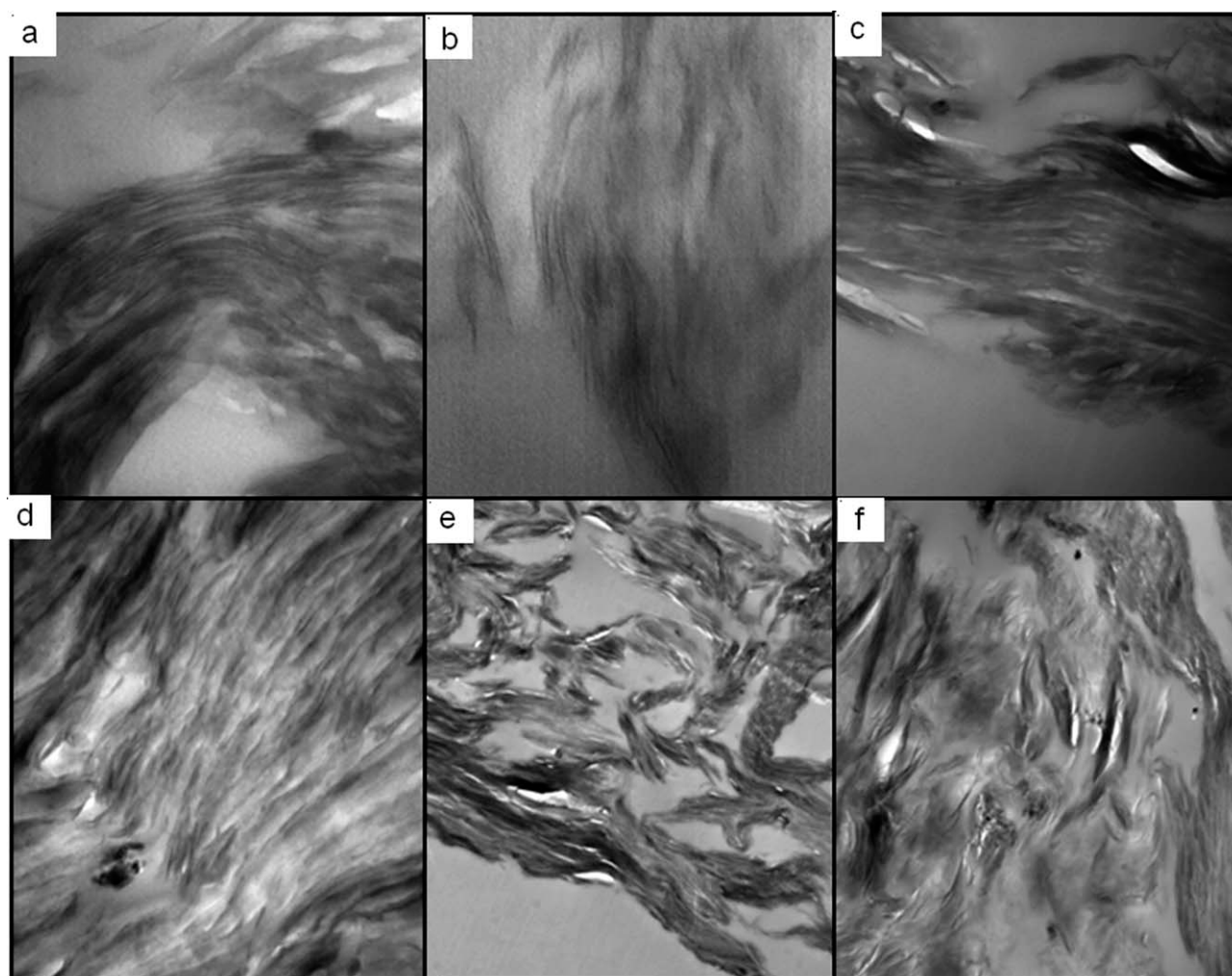


Figure 7 TEM micrographs of different composites (a) NWC5, (b) NWC10, (c) NWC20, (d) CL5, (e) CL10, and (f) CL20.

silicates and WF that may have decreased its nucleating effect.^{25,26} Thus, the chain mobility in NWC5 was reduced due to better wetting with the polymer matrix than with the other samples.

Because cellulose is a crystalline material with structures and properties that can change, the structure and properties of cellulose composites may also change. XRD scans were acquired from 10 to 40° to monitor the changes in crystalline structure in the

filler and the host matrix (Fig. 6). Diffraction in the matrix at 14.2°, 16.3°, 18.60°, and 21.2° was attributed to the 110, 040, 130, and 111 crystal planes of the

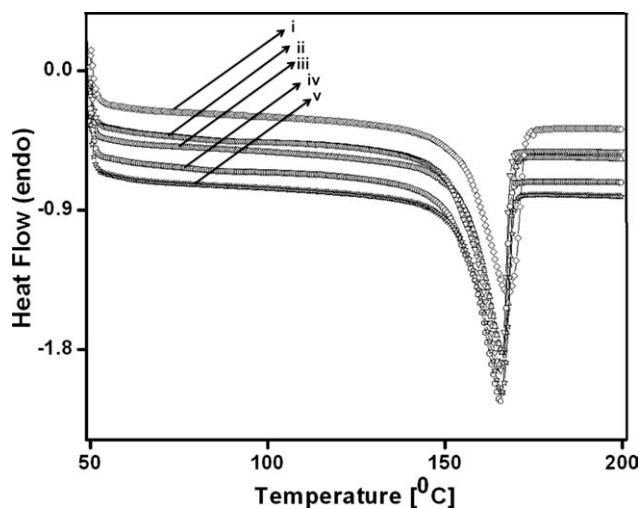


Figure 8 DSC thermograms of composites showing the variation in melting temperature (i, ii, iii, iv, and v represents NWC5, 10, 20, CL 10, and PP, respectively).

TABLE II
DSC Characteristics of Composites

Samples	T_m [°C]	ΔH_m [J/g]	T_c [°C]
PP	164	80	110
NWC5	169	78	116
NWC10	166	72	119
NWC20	165	71	118
WF5	162	70	118
WF10	161	68	117
WF20	160	67	119
CL5	164	79	110
CL10	163	77	111
CL20	160	74	109

monoclinic nature α -form, respectively,²² which did not change in the composites up to 20% filler concentrations. There have been reports on the generation of an additional peak at 16.2° in the XRD spectrum that corresponds to the 300 diffraction plane for the β -form of PP crystals with a hexagonal configuration after incorporation of sisal fibers. However, no β -modification was detected in the neat matrix or the composites in this study.²⁸

Mechanical properties

Mechanical property measurements are shown in Figures 9(a,b). They depended on the amount of filler inside the polymer matrix. The stiffness of the composites increased linearly with increasing filler content in the matrix for certain composites. There may have been orientation effects in which reinforcing phases oriented toward the direction of the load and increased stiffness. The tensile strength of CLs decreased drastically and it was attributed to the lack of interaction between the host matrix and the filler. The reduction in CLs mechanical properties was greater than that of WFCs, which was attested to the presence of increased attraction through electrostatic bonding between MA-grafted polymer chains and hydroxyl groups in WF. The strength was markedly higher in NWC5 than in other samples. It was assumed that interfacial adhesion in these samples was similar to WF5 and WF10, and the only difference was the existence of silicate layers in the matrix. Because silicate layers were not compatible with the host matrix due to highly hydrophobic nature of polymer, the extent of dispersion of the fillers in the matrix must have been responsible for the higher strength in NWC5. This was confirmed by TEM analysis in which a delaminated structure was observed. The use of functionalized polymers is advantageous for improved tensile strength in PP-wood composites due to interaction between the functionalized fraction and cellulose. Furthermore, as soon as the loading increased, aggregation also increased, decreasing the elongation of the composites, as shown in Figure 9. Only NWC5 was similar to the neat matrix. When the content of particles in the composites increased, they touched each other and generated large bundles that could not carry a sufficient external load and fell apart. In addition, the stress transfer from one phase to another became difficult and produced a product with poor mechanical properties. To evaluate the effect of functionalization on strength, composites consisting of 10% MA-grafted polymers were examined (i.e., the amount of grafted polymer was 10% in NWC5). The tensile strength of this composite was 36.5 MPa (average of five samples), which was not significantly different from NWC 5 (5% compatibil-

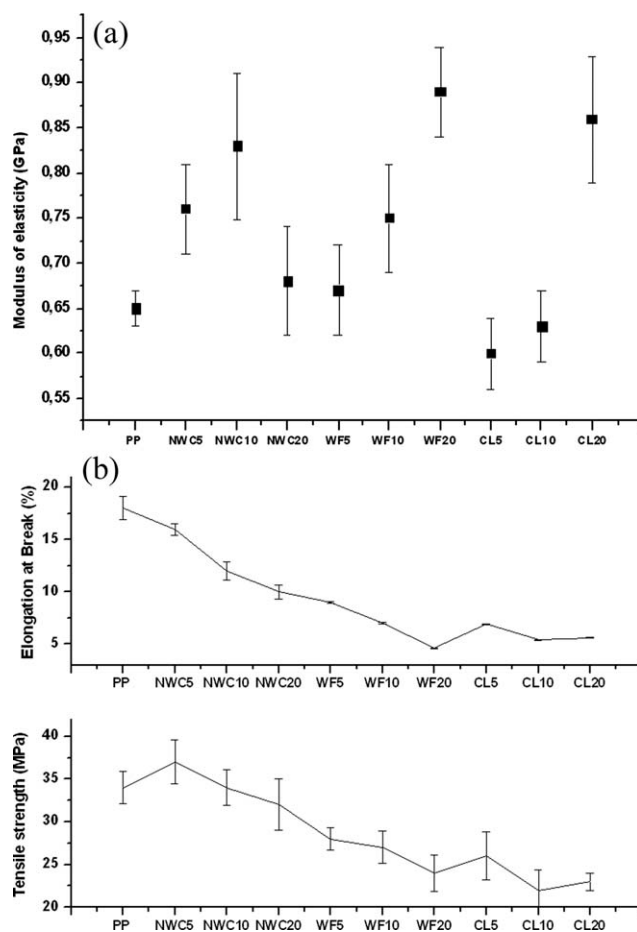


Figure 9 (a) Modulus of Elasticity for different composites. (b) Elongation at break and tensile strength for different composites.

izer). Previous studies showed that strong interaction by chemical bonding between hydroxyl groups in cellulose and the functionalized host matrix increased with increasing functionality, resulting in increased polymer strength.^{2,21,25} This was not detected in this study because of a limited number of hydroxyl groups in the cellulose-modified clay; hydroxyl groups were not available for chemical bonding with anhydride due to bonding with layered silicates. Thus, modified layered silicates were responsible for higher dispersion and competitive strength in composites with smaller amounts of functionalized polymer. Furthermore, larger amounts of MA are not advisable in composites during melt blending due to the possibility of matrix degradation through Norrish-I and Norrish-II free radical reactions that cause matrix fragmentation.²⁹

Surface morphology

The presence of hydroxyl groups on the surface of cellulose fibers make it hydrophilic and increase the surface energy, whereas polymer matrices have a

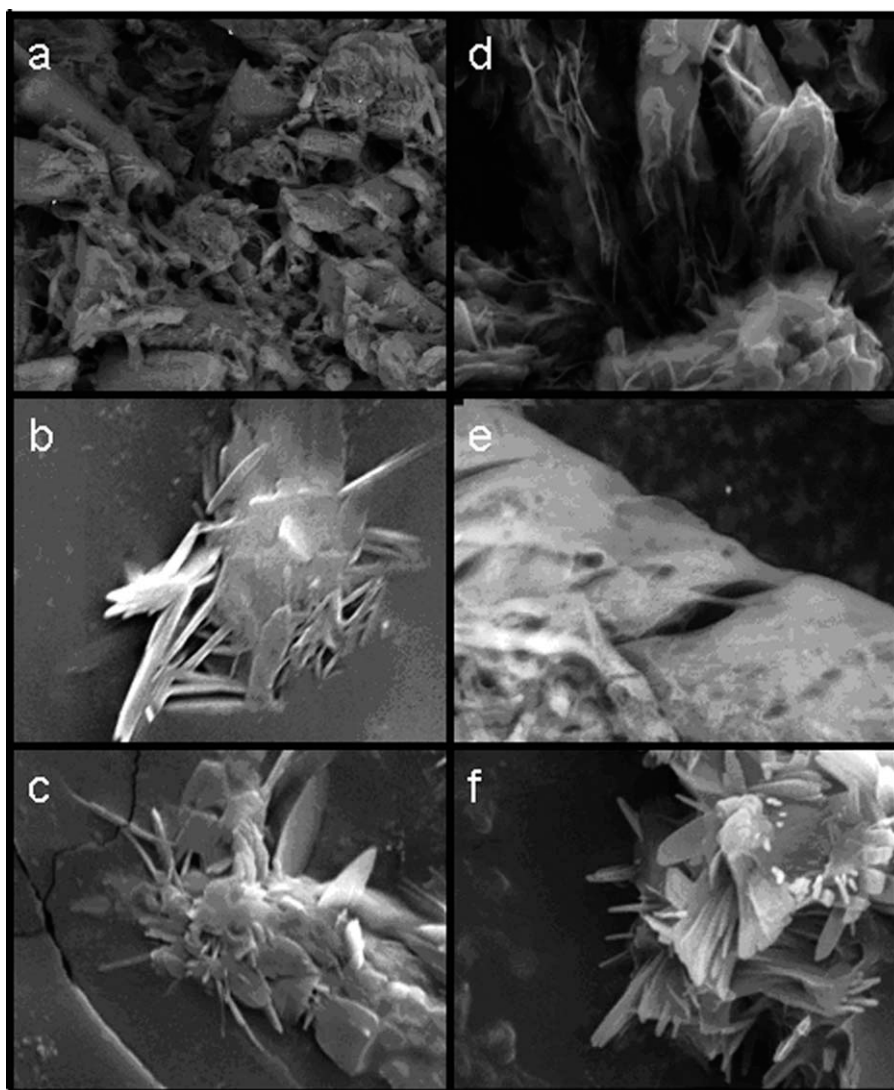


Figure 10 SEM micrographs of composites (a) NWC5, (b) CL20, (c) NWC20, (d) CL5, (e) NWC5, and a different portion of the sample (f) WF20.

modest cohesive energy and a strong hydrophobic nature. To increase the bonding at the interface, the polymer was functionalized by MA, with the expectation of the reinforced, high bond strength phase. SEM micrographs of the surface are shown in Figure 10(a–e). In this study, typical SEM images showed large gaps and voids on the surface, indicating poor interfacial adhesion between the reinforcing phase and the matrix. These results were consistent with the mechanical properties, because tensile strength decreased gradually with all fillers, except NWC5 and CL5 [Fig. 10(a,d)]. Aggregated clumps of fillers were observed for CL20, NWC20 and WF20 [Fig. 10(b,c,f)], indicating noncompatibility with the polymer matrix or absence of intramolecular bonding. The macroparticles of agglomerated fillers concentrated stress, initiating and propagating cracks in the matrix that can result in complete failure. The cracks around the large cluster of particles in Figure

10(c) for NWC20 confirmed that the matrix failed, due to poor dispersion and compatibility, preventing a smooth stress distribution from the filler to the matrix. Based on quantitative modeling, Dányádi et al.⁴ suggested that interfacial adhesion was an important factor in determining composite properties, the amount of functionalized polymer had an optimum and the processing conditions and resulting structure also affected the performance of the composites. The circular crack propagation observed in the SEM micrographs of NWC5 [Fig. 10(e)] indicated that slow failure of the matrix occurred during loading. This was supported by the higher tensile strength of this sample, due to proper distribution of the filler.

CONCLUSIONS

This study developed fillers with synergetic properties between microcrystalline cellulose and clay.

Agglomeration increased with increasing filler concentration, due to better interaction between clay and cellulose that promoted random accumulation of silicate tactoids. Dispersion was better at lower concentrations, attributed to the availability of a greater amount of functional groups from MA-grafted polymer chains in these samples. Because the mechanical properties improved at lower filler loadings, uniform dispersion of fillers was considered more important than the filler concentration in the host matrix. In conclusion, microcrystalline cellulose-modified clay may be useful for improving the mechanical properties of composites at certain filler concentrations and preventing phase separation that results in poor performance. The bond strength between fibers and the polymer matrix depended on the chemical/molecular interactions, atomic composition, and topographical nature of the fiber surface, which was influenced by modification of fibers or the polymer matrix.

J.K.P. is grateful for Japan Society for Promotion of Sciences (JSPS) for providing fellowship during completion of the manuscript. Authors gratefully acknowledge the ERC (Micro-Thermal System Research Center), Second Stage of Brain Korea 21 of Seoul National University and Japan Society for Promotion of Science.

References

- Pandey, J. K.; Ahn, A. H.; Lee, C. S.; Mohanty, A. K.; Misra, M. *Macromol Mater Eng* 2010, 295, 975.
- Pandey, J. K.; Kumar, A. P.; Misra, M.; Mohanty, A. K.; Drzal, L. T.; Singh R. P. *J Nanosci Nanotechnol* 2005, 5, 497.
- Mohanty, A. K.; Misra, M.; Drzal, L. T. *J. Polym Environ* 2000, 10, 19.
- Dányádi, L.; Janecska T.; Szabó, Z.; Nagy, G.; Móczó, J.; Pukánszky, B. *Compos Sci Technol* 2007, 67, 2838.
- Bledzki, A. K.; Gassan, J. *Prog Polym Sci* 1999, 24, 221.
- Miriam, M.; Lima, L.; Vorsali, R. *Macromol Rapid Commun* 2004, 25, 771.
- Candanedo, S. B.; Roman, M.; Gray, D. G. *Biomacromolecules* 2005, 6, 1048.
- Samir, M. A. S. A.; Alloin, F.; Dufresne, A.; *Biomacromolecules* 2005, 6, 612.
- Pandey, J. K.; Chu, W. S.; Kim, C. S.; Lee C. S.; Ahn, S. H. *Compos Part B Eng* 2009, 40, 676.
- Pandey, J. K.; Lee, J. W.; Chu, W. S.; Saini, D. R.; Mohanty, A. K.; Mishra, M.; Lan, T.; Ahn, S. H. *Nanocomposites of Polyolefins for Packaging Applications*, Chapter 4. In the book on *Polymer Nanocomposites for Packaging Application*; Nalwa, H. S., Mohanty, A. K., Eds.; American Scientific Publishers:Valencia, CA,2010.
- Lei, Y.; Wu, Q.; Clemons, C. M.; Yao, F.; Xu, Y. *J Appl Polym Sci* 2007, 106, 3958.
- Gao, F. *Mater Today* 2004, 7, 50.
- Hetzer, M.; Kee, D. D. *Chem Eng Res Design* 2008, 86, 1083.
- Thunwall, M.; Boldizar, A.; Rigdahl, M.; Banke, K.; Lindström, T.; Tufvesson, H.; Högman, S. *J Appl Polym Sci* 2008, 10, 918.
- Zhong, Y.; Poloso, T.; Hetzer, M.; Kee, D. D. *Polym Eng Sci* 2007, 47, 803.
- Park, H.; Misra, M.; Drzal, L. T.; Mohanty, A. K. *Biomacromolecules* 2004, 5, 2281.
- Petersson, L.; Oksman, K. *Compos Sci Technol* 2006, 66, 2187.
- Pandey, J. K.; Lee, J. W.; Chu, W. S.; Kim, C. S.; Lee, C. S.; Ahn, S. H. *Macromol Res* 2008, 16, 396.
- Cave, I. D.; Hutt, L. *Wood Sci Technol* 1968, 2, 268.
- Taiz, L.; *Ann Rev Plant Physiol* 1984, 35, 385.
- Helbert, W.; Sugiyama, J.; Ishihara, M.; Yamanaka, S. *J Biotechnol* 1997, 57, 29.
- Tserki, V.; Matzinos, P.; Kokkou, S.; Panayiotou, C. *Compos Part A* 36: 965 2005.
- Wang, N.; Ding, E.; Cheng, R. *Polymer* 2007, 48, 3486.
- Freudenberg, U.; Zschoche, S.; Simon, F.; Janke, A.; Schmidt, K.; Behrens, S. H.; Auweter, H.; Werner, C. *Biomacromolecules* 2005, 6, 1628.
- Ray, S. S.; Okamoto, M. *Prog Polym Sci* 2003, 28, 1539.
- Maiti, P.; Nam, P. H.; Okamoto, M.; Hasegawa, N.; Usuki, A. *Macromolecules* 2002, 35, 2042.
- Pandey, J. K. PhD Thesis, University of Pune, 2007.
- Zhou, X. P.; Li, Y.; Xie, X. L.; Tjong, S. C. *J Appl Polym Sci* 2003, 88, 1055.
- Pandey, J. K.; Reddy, R. K.; Kumar, A. P.; Singh, R. P. *Polym Degrad Stab* 2005, 88, 234.